

Internally biased PZT materials for high-power sonar transducers

David F. Waechter, S. Eswar Prasad, Richard G. Blacow and Bin Yan
Sensor Technology Limited, PO Box 97, Collingwood, ON Canada L9Y 3Z4

ABSTRACT

This paper examines the properties of three lead zirconate titanate (PZT) compositions that possess an internal bias field. The materials considered are Navy Type I, Navy Type III and a new composition called biased PZT (b-PZT). The latter was developed to achieve similarly low loss levels and similarly high internal bias field and coercive field as Navy Type III, but with higher piezoelectric charge coefficients. The three materials were characterized by measuring polarization vs. field as well as the displacement of multi-layer stack actuators. Field-induced crack propagation studies were also performed as a means to assess the relative robustness of the materials. In addition, the properties of barrel-stave flexensional transducers fabricated using the three materials were measured and compared. It is shown that the new b-PZT composition is a suitable substitute for Navy Type I and Navy Type III and may provide superior performance in high-power sonar transducers and other demanding applications.

1. INTRODUCTION

Hard PZT ceramics such as Navy Type I and Navy Type III are commonly used in high-power sonar transducers because of their low loss and high mechanical Q factor. The impurity additions that are commonly used in these ceramics introduce an internal bias field, which is made evident by a lateral shifting of polarization vs. field loops along the electric field axis. The internal field has been attributed to the introduction of acceptor impurity - oxygen vacancy complexes¹. The internal field increases the coercive field of the material and allows it to be driven with a higher electric field amplitude. In this respect the internal field plays a similar role as an externally applied DC bias, which can also increase the permissible electric field amplitude², but at the expense of more complex drive electronics.

The maximum permissible field in a sonar transducer is not straight-forward to define and generally involves leaving a suitable safety margin. In the case of disposable transducers, the field limit may be determined the electric field amplitude that would produce excessive heating in the device. This is often dictated by depolarization-related energy loss² and the coercive field of the material. However for non-disposable transducers, a lower field limit based on long-term reliability considerations may be appropriate. For Navy Type III ceramics, an electric field limit of 10V/mil (rms) has been chosen as an industry standard and is based on considerations of both reliability and acceptable losses³.

Unfortunately the same impurity additions that reduce losses and increase the internal bias field and coercive field also tend to decrease the piezoelectric charge coefficients. This partially mitigates the benefit of the higher electric field limit. While transition metal impurities are often used to provide the necessary acceptor-type doping in hard PZT ceramics, we have identified a non-transition metal impurity that provides increased internal bias field and lower loss but with less degradation of the piezoelectric charge constants⁴. A new composition based on this non-transition metal impurity has been developed and has been designated as BM200⁵ (hereafter referred to as b-PZT). In this work we present properties of this new composition that are relevant to the operation of high-power sonar transducers. Comparisons to Navy Type I (BM400) and Navy Type III (BM800) equivalents are also presented.

The experimental characterization techniques used in the study are described in Section 2. These include polarization vs. field studies as well as crack propagation studies. The latter are used to examine reliability limitations connected with high amplitude cyclic electric fields. Section 3 presents the results polarization vs. field measurements while section 4 presents the crack propagation studies. Section 5 presents displacement measurements for multi-layer stack actuators fabricated using the three ceramic materials. The same multi-layer stacks were subsequently used as

driving elements in barrel-stave flextensional transducers and the transducer characteristics are presented in section 6. A discussion of the results and conclusions are presented in section 7.

2. EXPERIMENTAL TECHNIQUES

PZT ceramic samples were fabricated using conventional ceramic fabrication techniques. Precursor oxide powders and chosen additives were combined and subjected to standard milling and calcining operations. This was followed by further milling, pressing, bisquing and firing. Surface machining was then performed and silver metallization was applied by screen printing and firing. The samples were poled at high voltage at elevated temperature.

Samples for polarization vs. field measurements were disk-shaped with 14 mm diameter and 0.4 mm thickness. The polarization measurements were performed using a modified Sawyer-Tower circuit⁶ with a suitable sampling capacitor. The samples were tested at room temperature under oil immersion to prevent arcing. The measurement system used for quasi-static measurements has been described previously⁷. This system was subsequently upgraded by adding a higher speed data acquisition card so that measurements up to 1kHz could be performed. In addition, the control software was modified so that it was possible to measure P vs. E loops with a DC bias voltage so that $V_{max} > |V_{min}|$. In a typical measurement sequence, low voltage sweeps between V_{min} and V_{max} were performed for approximately 2s and the data from the final sweep was recorded. The voltage amplitude was then increased and the measurement was repeated for the new amplitude. For each amplitude numerical integration was performed to determine the area in the hysteresis loops. For high dielectric constant materials the polarization is approximately equal to electrical displacement and the loop area gives energy loss per unit volume⁸. Plots of energy loss as a function of electric field amplitude show a rapid rise when depolarization effects begin to appear in the negative field region of the polarization vs. field loops⁴.

Samples for crack propagation studies were fabricated using a rectangular geometry having dimensions 12.7mm x 3mm x 1.27mm. The 12.7mm x 3mm faces were screen printed with silver paste to form electrodes, as shown in Fig. 1. The same electrodes were also used to pole the specimens. The upper 1.27mm x 12.7mm face of each specimen was polished to a smooth finish with silicon carbide paper and then indented with a Vickers diamond pyramid, using a load of 20 N, applied for a period of 10 sec. The diamond shaped indent was aligned so that one set of corners was parallel, and the other normal, to the electrodes, as shown in the figure. The indentation process typically causes cracks in the vicinity of 200-300 μ m in length to emanate from the corners of the indent. In a typical experimental study cracks oriented parallel to the electrodes (i.e. normal to the applied field) are observed to grow under the influence of cyclic electric fields^{9,10}. Resistance to such propagation indicates that the material is more robust and is a desirable property for transduction materials used in high-power sonar transducers. In this work, the effect of crack propagation from the indent site was monitored by measuring changes in the LTE mode of the sample's impedance spectrum.

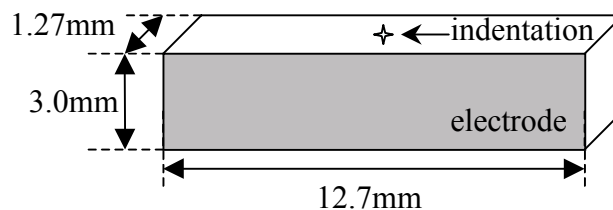


Figure 1. Indented ceramic sample for crack propagation studies.

The performance of the piezoelectric materials in barrel-stave flextensional transducers was characterized by measuring small signal impedance spectra as well as the high-power sound pressure levels (SPL). The latter results were measured up to a depth of 122m (400 feet) at the NUWC sonar test facility in Dresden, NY. The transducers were Class I devices according to the Brigham-Royster classification scheme¹¹ and have been described previously¹². A cutaway view is shown in Fig. 2. The transducers use a multi-layer piezoelectric stack of ring-shaped elements to excite a flexural

resonance of six aluminum staves that are mounted around the periphery, as shown. The stacks are pre-stressed by a bolt inserted through the center of the rings and are further stressed when the transducer is exposed to high water pressure. A neoprene rubber boot (not shown) provides a water-tight seal. The transducers have a low frequency broadband resonance near 1500Hz. Six transducers were fabricated for the study, two each using Navy Type I, Navy Type III and b-PZT ceramics. Prior to attaching the staves and rubber boot, the vertical displacement of the pre-stressed ring stacks shown in the figure were measured using an LVDT-based strain measurement system⁷.

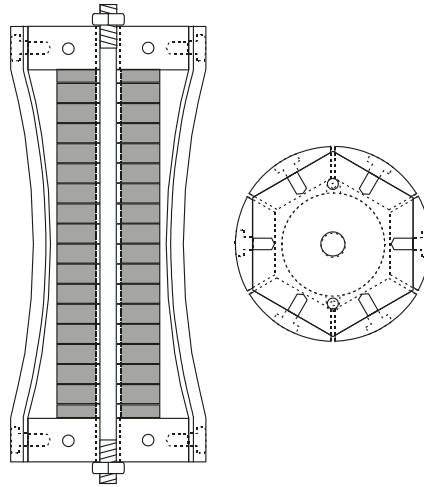


Figure 2. Cutaway view of flexensional transducer used in the study.

3. POLARIZATION vs. FIELD RESULTS

Quasi-static polarization vs. field loops measured with large electric field amplitude for Navy Type I, Navy Type III and bPZT are shown in Fig. 3. For each material the horizontal center of the loops is offset from the $E=0$ axis, indicating the presence of an internal bias field. The internal bias field for Navy Type I is 0.42MV/m, while those for Navy Type III and b-PZT are larger and close to each other (0.61MV/m and 0.66MV/m respectively). The coercive fields progress in the same order from low to high for the three materials and are 1.63MV/m for Type I, 1.88MV/m for Type III and 1.94MV/m for b-PZT. The spontaneous polarization is similar for Types I and III and smaller for b-PZT.

Fig. 4 shows the energy loss per unit volume, deduced from the area of quasi-static P vs. E loops, as a function of electric field amplitude. The figure shows that energy loss rises rapidly as the peak electric field approaches the coercive field of the given material.

Fig. 5 shows the energy loss per unit volume, deduced from the area of 1kHz P vs. E loops, as a function of electric field amplitude. In this case the figure focuses mainly on fields near and below the coercive field and results are shown for different values of externally applied DC bias, oriented in line with the original poling direction. The results show that the energy loss is highest for Navy Type I and that externally applied DC bias can noticeably lower the energy loss of this material in the high field region. However the reduction observed for Navy Type I still does not bring the energy loss close to that of either non-externally biased Navy Type III or b-PZT, even when the external bias on the Navy Type I is larger than the difference in the internal bias fields of the respective materials. This suggests that internal bias fields, while often present in low loss materials, are not a significant contributing factor to the lower loss, at least in the low and medium field regime. Losses in piezoelectric materials are usually attributed to domain mechanisms^{13, 14}. Because of their larger coercive fields, the losses in Navy Type III and b-PZT, shown in Fig. 5, have only a very small dependence on the external DC bias field for the electric field range shown.

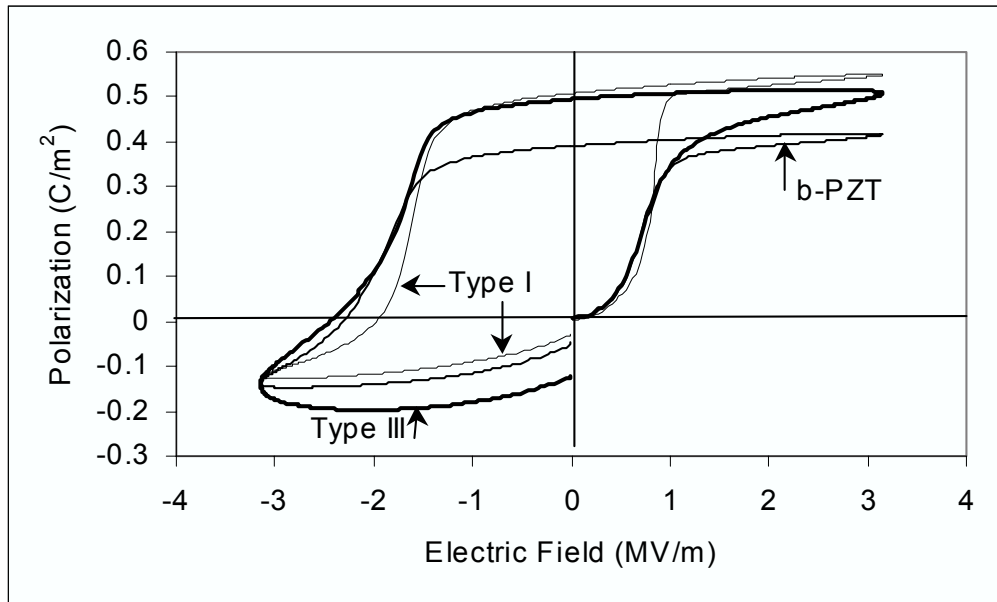


Figure 3. Quasi-static polarization vs. field loops for Navy Type I, Navy Type III and b-PZT ceramics.

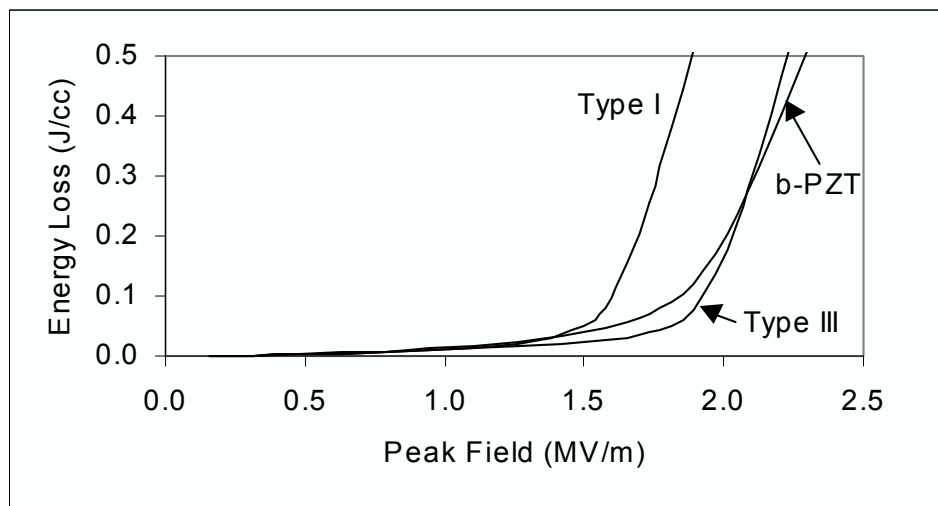


Figure 4. Energy loss per unit volume as a function field amplitude deduced from quasi-static P-E loops for Navy Type I, Navy Type III and b-PZT ceramics.

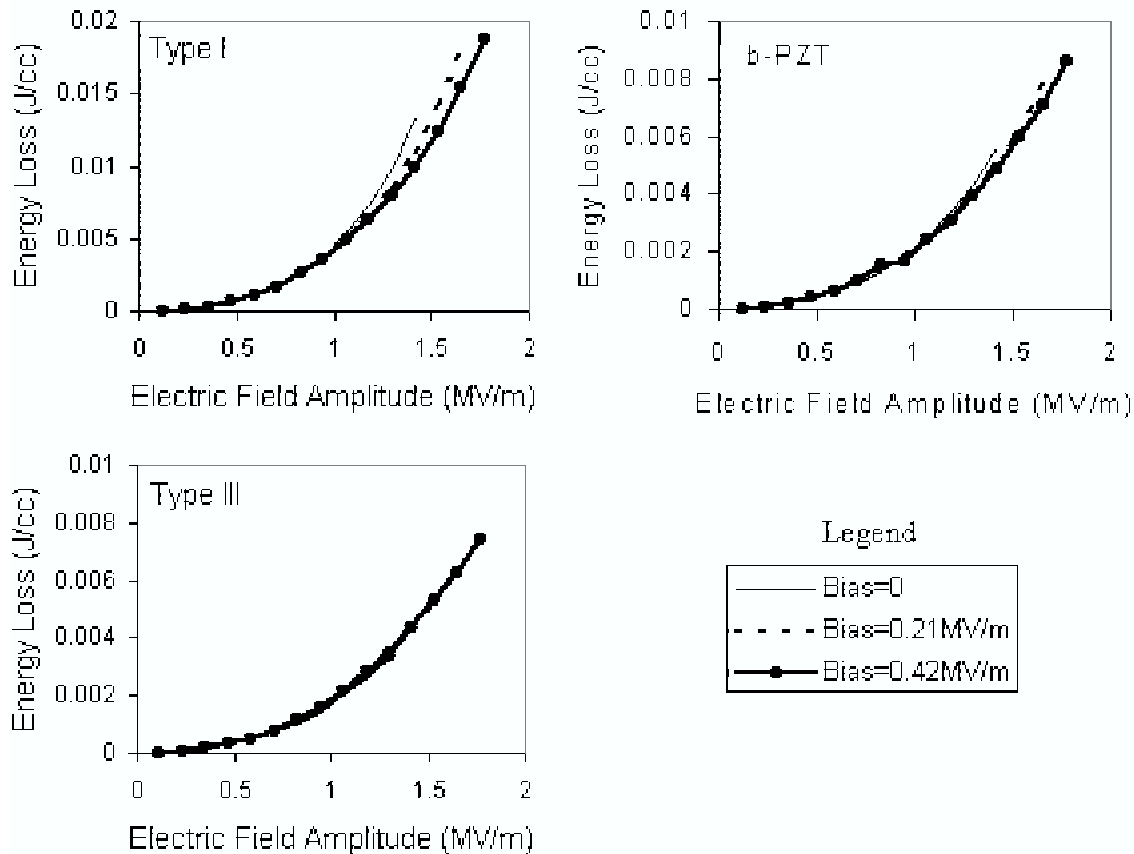


Figure 5. Energy loss per unit volume as a function field amplitude deduced from 1kHz P-E loops with different values of externally applied positive DC bias for Navy Type I, Navy Type III and b-PZT ceramics.

4. CRACK PROPAGATION RESULTS

Fig. 6 shows the impedance spectra for the LTE mode of indented bar samples measured after exposure to a 2Hz sine wave voltage sweep of 4000V peak amplitude for the shown number of cycles. This corresponds to a peak field of 3.15MV/m, which is substantially larger than the coercive field of the materials. For all materials the impedance spectra peaks were shifted to lower frequencies and decreased in magnitude for increasing numbers of cycles. Tests performed on non-indented samples suggest that these changes are connected with damage propagation from the indentation site. Non-indented samples of Navy Type III and b-PZT that were exposed to the same electric field amplitude exhibited only minimal change in their impedance spectra for as many as 5000 cycles. Non-indented Navy Type I samples were also more robust than their indented counterparts, but showed significant change with as few as 100 cycles.

The Fig. 6 results show that for the chosen electric field, Navy Type I was the least robust and showed the largest resonance frequency shift and impedance peak reduction with the fewest number of stress cycles. Biased PZT appears to be slightly more robust for the chosen field than Navy Type III, retaining larger peaks with less frequency shift for 100 and 200 cycles. Compared to Navy Type III, the progression of the spectra for an increasing number of cycles was more orderly in the case of b-PZT, suggesting the presence of a continuous rather than "stop-and-go" propagation of the associated defect structure. Similar observations were made in several tested samples.

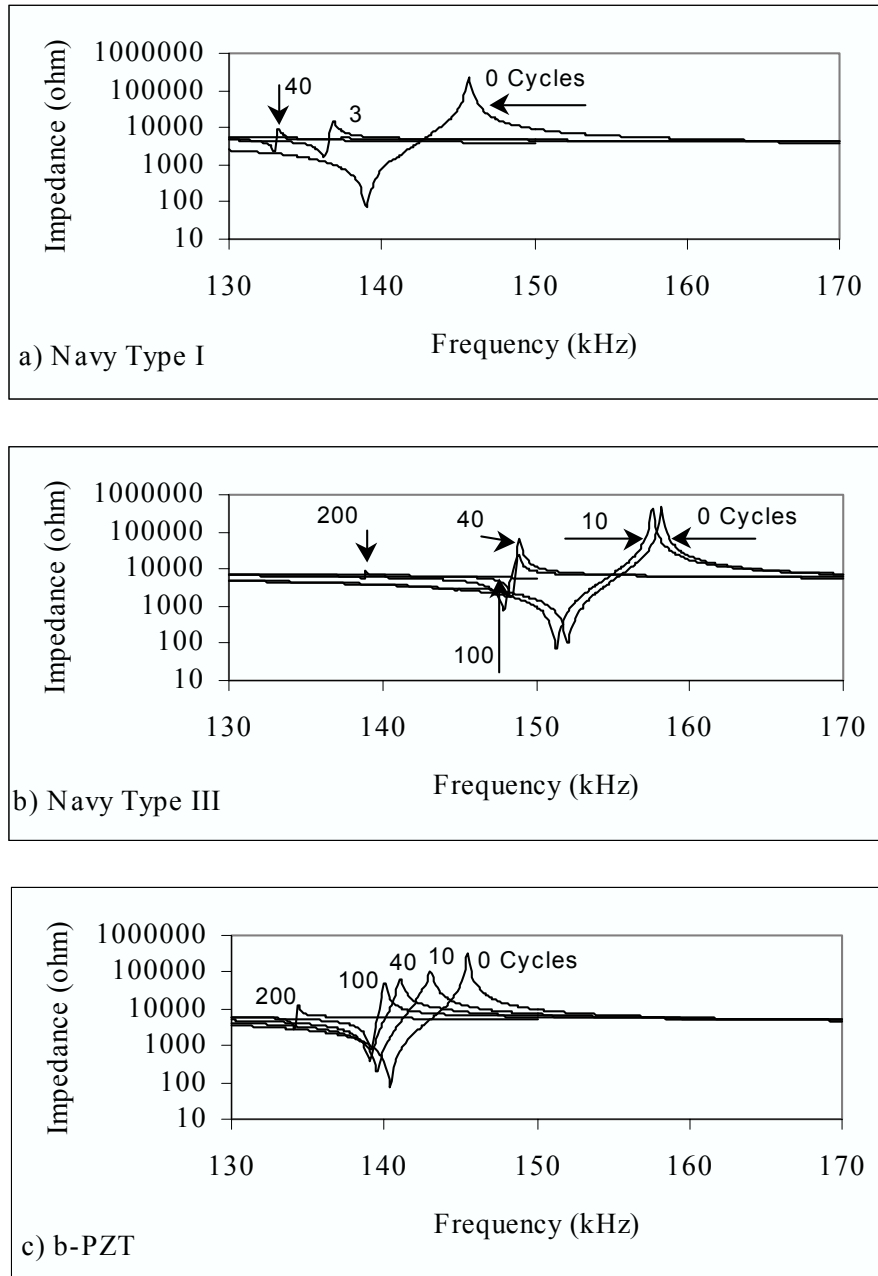


Figure 6. Impedance spectra progression for increasing numbers of electric field stress cycles at 3.15MV/m for indented bar samples of a) Navy Type I, b) Navy Type III and c) b-PZT ceramics.

5. MULTI-LAYER STACK CHARACTERIZATION

Displacement vs. voltage characteristics were measured for the multi-layer stack actuators that were later used in the fabrication of barrel-stave flextensional transducers. The stacks were tested with a central pre-stress rod in place, as shown in Fig. 2, but prior to attaching the staves and rubber boot. The displacement vs. voltage characteristics for stacks using Navy Type I, Navy Type III and b-PZT ceramic elements are shown in Fig. 7. The results show that b-PZT

yields a displacement that is higher than that of Navy Type III but not quite as high as that of Navy Type I. As was noted in section 3, the loss levels of b-PZT are similar to those of Navy Type III but the low loss has now been achieved with less degradation of the strain characteristics. d_{33} values measured by the Berlincourt technique are typically ~220 pC/N for Navy Type III, 300pC/N for Navy Type I and 250 pC/N for b-PZT.

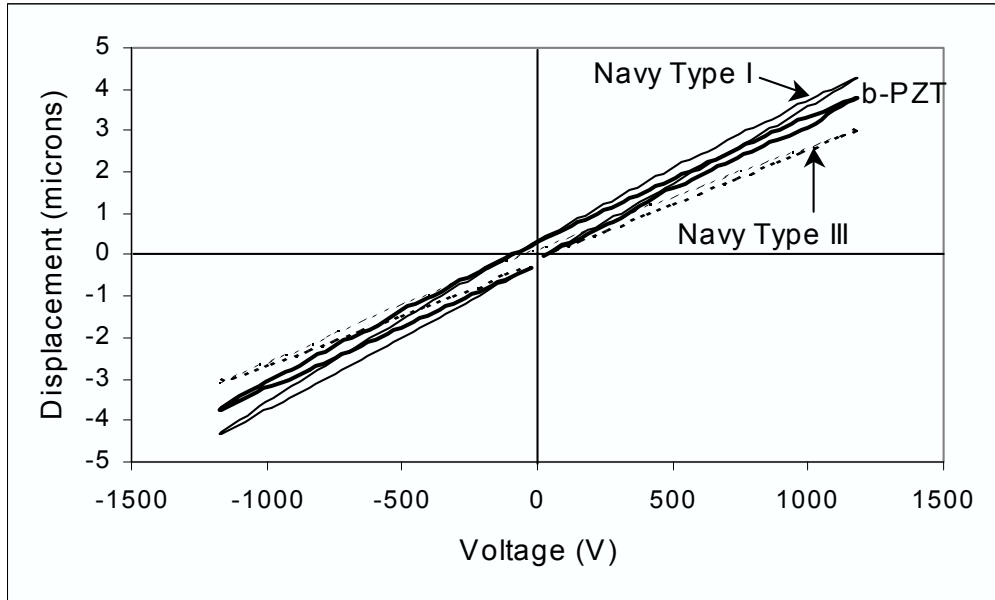


Figure 7. Displacement vs. voltage for pre-stressed multi-layer stack actuators used in barrel-stave flextensional transducers.

6. TRANSDUCER CHARACTERIZATION

The impedance spectra of the barrel stave flextensional transducers were measured in shallow water near the lowest frequency flextensional mode. These spectra were well fit by the Van Dyke equivalent circuit model shown in Fig. 8. Table 1 shows the resulting equivalent circuit element values as well as the resonance frequencies. All circuit element values for b-PZT were intermediate between those of Navy Type I and Navy Type III. The resonance frequencies were all near 1500Hz regardless of the transduction material.

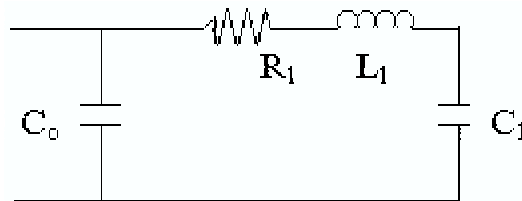


Figure 8. Van Dyke equivalent circuit model of piezoelectric resonator.

Table 1. Parameters of Van Dyke equivalent circuit model and resonance frequencies of six barrel-stave flextensional transducers in shallow water.

	C_o (nF)	C_1 (nF)	L_1 (H)	R_1 (k Ω)	F_r (Hz)
Navy Type I	19.4	0.96	12.1	9.5	1474
Navy Type I	19.6	1.03	10.2	6.5	1548
Navy Type III	13.7	0.48	23.3	20.9	1507
Navy Type III	13.4	0.47	24.9	23.1	1470
b-PZT	16.1	0.82	14.1	11.2	1486
b-PZT	15.9	0.69	16.2	13.2	1505

Transducer sound pressure levels for an operating voltage of $400V_{rms}$ and a depth of 122m are shown as a function of frequency in Fig. 9. As expected from the above results, the curves for the b-PZT transducer lie between those of the Navy Type I and Navy Type III transducers. The mechanical Q factor of the b-PZT transducer, indicated in the figure, is also intermediate. The resonance frequencies are larger than those shown in Table 1 because of the depth dependence of this quantity.

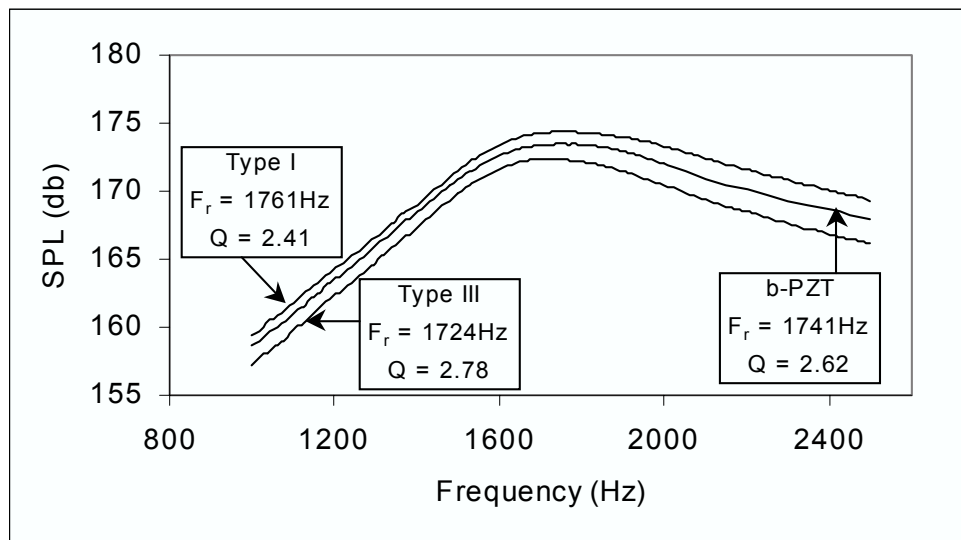


Figure. 9. Sound pressure levels as a function of frequency at 122m depth for transducers fabricated using Navy Type I, Navy Type III and b-PZT. The operating voltage was $400V_{rms}$.

Fig. 10 shows the peak SPL for the transducers at the same depth. In fig. 10a the results are shown as a function of rms drive voltage and, once again, the b-PZT curves are intermediate between those of Navy Type I and Navy Type III. However when the same curves are plotted as a function of real input power (fig. 10b) the curves are nearly coincident. This shows that the power conversion efficiency at these power levels was nearly the same for each transducer and was dominated by loss factors apart from the transduction material. Power efficiency values were approximately 40%.

7. DISCUSSION AND CONCLUSIONS

The new biased PZT material has been shown to retain the low loss and high coercive field of Navy Type III while providing higher strain. Transducers fabricated using the new material have electrical impedance characteristics that are intermediate between those using Navy Type I and those using Navy Type III. The crack propagation studies

suggest that b-PZT is at least as robust as Navy Type III for a given level of electric field stress. And since d_{33} is larger for b-PZT, this also suggests that b-PZT may be robust than Navy Type III for a given level of cyclic induced strain. The results further suggest that both b-PZT and Navy Type III are more robust than Navy Type I for a given level of electric field stress. However the present results do not show whether they are more robust for a given level of induced strain since d_{33} is highest for Navy Type I and consequently these samples experienced greater strain in the crack propagation studies. Additional work is required to better establish reliability-based field and output power limits for each material in a given transducer application.

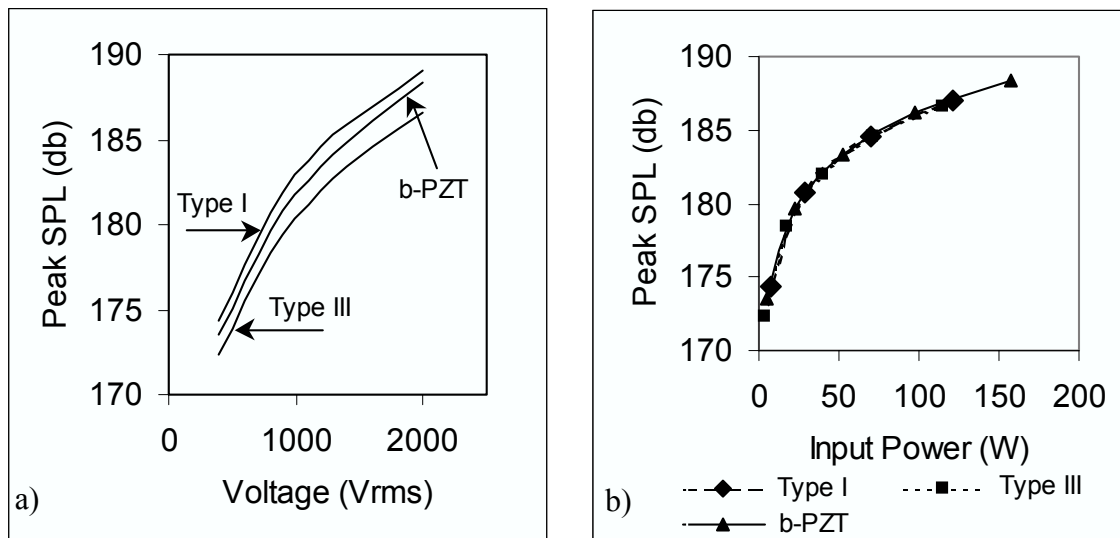


Figure 10. Peak sound pressure levels at a 122m depth for transducers fabricated using Navy Type I, Navy Type III and b-PZT, as a function of a) rms voltage and b) real input power.

ACKNOWLEDGMENT

Funding for this work was provided in part by the Department of National Defence (Canada) and the Office of Naval Research (USA). We thank D. Jones (DRDC) and J. Lindberg (ONR) for their support.

REFERENCES

1. S. Takahashi, "Internal bias field effects in lead zirconate-titanate ceramics doped with multiple impurities", *Jpn. J. Appl. Phys.*, **20**, 95-101, 1981.
2. M.B. Moffett, M.D. Jevnager, S.S. Gilardi and J.M. Powers, "Biased lead zirconate titanate as a high-power transduction material", *J. Acoust. Soc. Am.*, **105**, 2248-2251, 1999.
3. D.F. Jones and J.F. Lindberg, "Recent transduction developments in Canada and the United States", *Proc. Institute of Acoustics*, **17**, Part 3, 15-33, 1995.
4. D.F. Waechter, S.E. Prasad and R. Blacow, "Biased PZT materials for acoustic transducers", *Proc. ICONS 2002, International Conference on Sonar – Sensors and Systems*, Eds. H.R.S. Sastry, D.D. Ebenezer and T.V.S. Sundaram, 665-672, Allied Publishers, Kochi, India, 2002.
5. www.sensortech.ca.
6. C.B. Sawyer and C.H. Tower, "Rochelle Salt as a Dielectric", *Phys. Rev.*, **35**, 269-273, 1930.
7. B. Yan, D. Waechter, R. Blacow and S. E. Prasad, "Measurement of strain and polarization in piezoelectric and electrostrictive actuators", *Proc. 2nd Canada-US CanSmart Workshop on Smart Materials and Structures*, Ed. G. Akhras, 33-39, Montreal, 2002.

8. K. Uchino and S. Hirose, "Loss mechanisms in piezoelectrics", *IEEE Trans. UFFC*, **48**, 307-321, 2001.
9. S. Ferguson, H.W. King, D.F. Waechter, R. Blacow and S.E. Prasad, "Crack growth in lead magnesium niobate - lead titanate ceramics by cyclic electric fields", *Proc. SPIE Smart Structures and Materials Conf.*, **5387**, 513-518, 2004.
10. H. Cao and A.G. Evans, "Electric-field-induced fatigue crack growth in piezoelectrics", *J. Amer. Ceram. Soc.*, **77**, 1783-1786, 1994.
11. G.A. Brigham and L.H. Royster, "Present status in the design of flextensional underwater acoustic transducers," *J. Acoust. Soc. Am.*, **46**, 92-98, 1969.
12. S.E. Prasad, R. Blacow, J. Frank and D. Waechter, "Deployable sonar systems for underwater communications", *Proc. Int. Conf. on Sonar-Sensors & Systems (ICONS-2002)*, 119-126, Allied Publishers, Kochi, India, 2002.
13. S. Takahashi and M. Takahashi, "Effects of impurities on the mechanical quality factor of lead zirconate titanate ceramics", *Jpn. J. Appl. Phys.*, **11**, 35-39, 1972.
14. A.V. Mezheritsky, "Elastic, dielectric, and piezoelectric losses in piezoceramics: how it all works together", *IEEE Trans. UFFC*, **51**, 695-707, 2004.